

# JGR Space Physics

## RESEARCH ARTICLE

10.1029/2024JA033238

### Key Points:

- Lower hybrid drift wave type depends on the electron beta: as electron beta increases, these waves become more electromagnetic in nature
- The energy transfer is higher in electrostatic waves and, on average, primarily in the parallel direction relative to the magnetic field
- Linear dispersion theory shows electrostatic waves are perpendicular propagating while electromagnetic waves propagate in oblique direction

### Correspondence to:

N. Ahmadi,  
Narges.Ahmadi@colorado.edu

### Citation:

Ahmadi, N., Ji, H., Yoo, J., Ergun, R., Thomas, I., Banka, R., et al. (2025). Properties of lower hybrid drift waves and energy transfer near and inside the magnetic reconnection electron diffusion regions. *Journal of Geophysical Research: Space Physics*, 130, e2024JA033238. <https://doi.org/10.1029/2024JA033238>

Received 28 AUG 2024  
Accepted 24 MAR 2025

### Author Contributions:

**Conceptualization:** Hantao Ji, Robert Ergun  
**Data curation:** Jongsoo Yoo  
**Formal analysis:** Hantao Ji, Jongsoo Yoo, Izzy Thomas, Rahul Banka, Emma Schultz-Stachnik, Alma Alex  
**Funding acquisition:** Hantao Ji  
**Investigation:** Hantao Ji, Jongsoo Yoo, Robert Ergun, Emma Schultz-Stachnik, Alma Alex  
**Methodology:** Hantao Ji, Izzy Thomas, Rahul Banka  
**Project administration:** Hantao Ji  
**Resources:** Jongsoo Yoo  
**Software:** Jongsoo Yoo  
**Supervision:** Hantao Ji  
**Validation:** Hantao Ji, Jongsoo Yoo, Robert Ergun  
**Writing – original draft:** Hantao Ji, Izzy Thomas  
**Writing – review & editing:** Hantao Ji, Jongsoo Yoo, Izzy Thomas, Rahul Banka

## Properties of Lower Hybrid Drift Waves and Energy Transfer Near and Inside the Magnetic Reconnection Electron Diffusion Regions

Narges Ahmadi<sup>1</sup> , Hantao Ji<sup>2</sup> , Jongsoo Yoo<sup>2</sup> , Robert Ergun<sup>1</sup> , Izzy Thomas<sup>3</sup> , Rahul Banka<sup>4</sup> , Emma Schultz-Stachnik<sup>5</sup>, and Alma Alex<sup>6</sup>

<sup>1</sup>Laboratory of Atmospheric and Space Physics, University of Colorado Boulder, Boulder, CO, USA, <sup>2</sup>Princeton Plasma Physics Laboratory, Princeton, NJ, USA, <sup>3</sup>Department of Physics, University of California San Diego, San Diego, CA, USA, <sup>4</sup>Department of Physics, Auburn University, Auburn, AL, USA, <sup>5</sup>Mathematics and Physics, University of Wisconsin-Parkside, Kenosha, WI, USA, <sup>6</sup>Department of Physics, Yale University, New Haven, CT, USA

**Abstract** We investigate properties of lower hybrid drift waves (LHDWs) near and inside the electron diffusion regions in 17 magnetopause and 9 magnetotail reconnection events using Magnetospheric MultiScale (MMS) mission observations. Our analysis show that LHDW type depend on the electron beta, as electron beta increases LHDWs become more electromagnetic in nature. The energy transfer from electromagnetic fields to particles is higher in electrostatic LHDWs and it is largely in parallel direction with respect to the local magnetic field. Linear dispersion analysis shows that electrostatic LHDWs are perpendicular propagating while electromagnetic waves propagate in oblique directions and the normalized wavenumber of all LHDW types falls within 0.5–0.8 range. A simple estimate on the LHDW nonlinear saturation suggests a possibly important roles played by these waves in supporting the reconnection electric field.

**Plain Language Summary** Magnetic reconnection is a fundamental process which converts magnetic energy into particle energy. In magnetic reconnection regions, large amplitude waves are frequently observed. One of these waves are called Lower Hybrid Drift Waves or LHDWs. LHDWs display quite different characteristics depending on their locations in terms of plasma parameters and can impact energy conversion in reconnection regions. In this paper, we use MMS observations and a local linear theory to investigate the LHDW properties near the reconnection sites. Our results show that the LHDWs type depends on plasma parameters and they can transfer large amount of energy to particles near reconnection sites.

## 1. Introduction

Magnetic reconnection, the breaking and rejoining of non-parallel magnetic field lines at the intersection of inflowing plasmas, is a source of abundant free energy that energizes particles. Magnetic reconnection is observed throughout the universe (Ji & Daughton, 2011) ranging from Earth's magnetosphere, to the Sun, to more distant astrophysical objects, and also in fusion plasmas. It is considered to be responsible for many energetic phenomena (Yamada et al., 2010) such as the ejection of large amount of mass from the solar surface and electron acceleration to produce the aurora.

One of the outstanding questions for magnetic reconnection is how does magnetic field energy efficiently dissipate into plasma. There have been numerous mechanisms proposed to energize plasma based on magnetized particle motion (Ji et al., 2022), such as Fermi reflection (Drake et al., 2006). Another often-mentioned candidate is different types of plasma waves and fluctuations which are frequently observed near the electron diffusion region (EDR) of the reconnection sites in space such as by the Magnetospheric Multiscale (MMS) mission or in the laboratory (Ji et al., 2023). Since the plasma in near-Earth space is essentially collisionless, it is natural to hypothesize that waves are generated by free energy in the current sheet and wave-particle interaction energizes particles.

In particular, lower-hybrid drift waves (LHDWs) are frequently observed during magnetic reconnection events. LHDWs are driven by a density gradient and also by perpendicular current or a relative drift between ions and electrons with a broadband frequency spectra around the lower hybrid frequency,  $f_{LH}$  (Davidson & Gladd, 1975).

The lower hybrid frequency  $f_{LH}$  is  $\left[ (f_{ci} f_{ce})^{-1} + f_{pi}^{-2} \right]^{-1/2}$  where  $f_{ci}$  is the ion cyclotron frequency,  $f_{ce}$  is the electron

cyclotron frequency and  $f_{pi}$  is the ion plasma frequency. In all the cases in this paper,  $f_{LH}$  is approximately  $(f_{ci}f_{ce})^{1/2}$ . LHDWs may be quasi-electrostatic (ES-LHDW) which are dominated by fluctuations in the electric field (Carter et al., 2001; Cattell & Mozer, 1986; Khotyaintsev et al., 2019; Yoo et al., 2020, 2024) or quasi-electromagnetic (EM-LHDW) with appreciable fluctuations in the magnetic field (Cozzani et al., 2021; Ji et al., 2004; Norgren et al., 2012; Shinohara et al., 1998; Yoo et al., 2020; Zhou et al., 2009). There are suggestions that ES-LHDW are excited at low plasma  $\beta$  while EM-LHDW at high plasma  $\beta$  (Carter et al., 2001; Ji et al., 2004; Yoo et al., 2020) ( $\beta$  is the ratio of plasma to magnetic pressure) but they are observed under various conditions (densities, temperatures and guide magnetic field strength) both in the magnetopause (Bale et al., 2002; Graham et al., 2019; Khotyaintsev et al., 2016; Yoo et al., 2020) and in the magnetotail (Cattell & Mozer, 1986; Chen et al., 2020; Cozzani et al., 2021; Norgren et al., 2012; Shinohara et al., 1998; Zhou et al., 2009). More recently, Wang et al. (2022) conducted a detailed study of 12 magnetotail reconnection events with detection of both ES-LHDW and EM-LHDW by focusing on their propagation characteristics and correlations with electrons quantities.

This study analyzes MMS data in an attempt to understand what determines the type of LHDW and their role in terms of magnetic energy dissipation during magnetic reconnection. Many prior studies of LHDW observations during individual magnetic reconnection events have been conducted. Here, however, a survey analysis of 26 LHDW observations near and inside the diffusion region for both magnetopause and magnetotail reconnection is performed. Plasma parameters are calculated and averaged over the fluctuation period interval. Fourier analysis is used to determine the power of electric and magnetic field fluctuations in the lower-hybrid frequency range. A correlation study between wave power, LHDW type,  $\beta_e$  and magnetic energy dissipation are conducted.

This paper is organized as follows: In Section 2, we review the data and methods used in the analysis. In Section 3, we present the results of correlation studies. Sections 4 and 5 show the results of linear dispersion analysis. Section 6 contains the summary and conclusions.

## 2. Data and Methods

In the present study 26 LHDWs events near and inside the EDR, observed by MMS1, have been selected to investigate the LHDWs properties and their impact on energy transfer between electromagnetic fields and particles. The EDR time was collected from previous studies (Wang et al., 2022; Webster et al., 2018). If the LHDW interval included the EDR time, the event is marked as inside the EDR and if it was outside of the EDR time, the event is near the EDR. 17 events were selected from Webster et al. (2018) in the magnetopause reconnection and 9 events from Wang et al. (2022) in the magnetotail reconnection with LHDW signatures. These events were selected based on clear LHDW signatures such as wave power within frequency range of  $[1, 2f_{LH}]$  and presence of fluctuations in electromagnetic fields. The LHDW intervals are loosely limited to the regions with electric field fluctuations selected by eye. Magnetic field data from the fluxgate magnetometer (FGM) instrument (Russell et al., 2016), electric field data from electric double probes (EDP) (Ergun et al., 2016; Lindqvist, 2016) as well as particle data from the Fast Plasma Investigation (FPI) (Pollock et al., 2016) were used to analyze the characteristics of LHDWs in each event. FPI ion measurements have the time resolution of 0.15 s, and electron measurements have the time resolution of 0.03 s.

Table 1 shows the list of the events and their properties based on plasma parameters measured by MMS1 data and dispersion analysis using Yoo et al. (2020). Event numbers marked by a star are the magnetotail events near and inside the EDR (events 18 to 26) and the rest of the table (events 1 to 17) is the LHDWs in the vicinity and inside of magnetopause EDRs. The events marked by superscript  $I$  are inside the EDR and the rest are near the EDR events. Table 1 contains the start and end time of the LHDWs, the electron beta ( $\beta_e$ ), the ratio of wave amplitude in magnetic field to electric field, the parallel energy transfer ( $\delta J_{\parallel} \delta E_{\parallel}$ ), the lower hybrid frequency ( $f_{LH}$ ) that are estimated using MMS1 data. The parallel and perpendicular directions are with respect to the background magnetic field. The table also includes the propagation angle (the angle between the wave vector and the background magnetic field) and wavenumber (normalized by electron gyro-radius) that are calculated using the dispersion code developed by Yoo et al. (2020). The dispersion analysis uses the plasma parameters measured by MMS1 as input to estimate the propagation angle and the wavenumber for each event. More details are provided in the dispersion relation analysis section of the paper. The plasma parameters from MMS measurements are averaged in each LHDW interval. For electromagnetic power calculations, we use burst electric field (8,192

**Table 1**  
Table of Numbered Magnetic Reconnection Events With LHDWs Observed Near and Inside the EDR

Event	Time interval (UTC)	$\beta_e$	$\frac{ B U_{\perp}}{ E }$	$\delta J_{\parallel} \delta E'_{\parallel}$ (nW/m <sup>3</sup> )	$f_{LH}$ (Hz)	$\theta^{\circ}$	$k\rho_e$
1	20151016/103324.0–103327.0	0.19	76	0.08 (64%)	18.5	88	0.58
2	20151016/130659.0–130702.0	0.56	156	0.45 (83%)	12.27	85	0.70
3	20151101/150802.0–150806.0	0.14	45	0.01 (70%)	24.30	88	0.61
4 <sup>I</sup>	20151206/233830.0–233833.0	0.18	109	0.07 (54%)	27.68	89	0.57
5 <sup>I</sup>	20151208/112043.0–112045.0	0.24	196	0.02 (69%)	18.67	87	0.57
6	20151209/010611.0–010614.0	0.67	254	0.12 (92%)	12.33	86	0.65
7	20151214/011740.0–011742.0	0.21	146	0.03 (53%)	19.14	90	0.47
8 <sup>I</sup>	20160110/091335.0–091339.0	0.12	57	0.12 (75%)	32.60	88	0.56
9 <sup>I</sup>	20160207/202334.0–202337.0	0.4	153	0.01 (83%)	13.31	88	0.66
10	20161022/125838.0–125841.0	0.29	120	0.27 (77%)	17.77	87	0.60
11 <sup>I</sup>	20161102/144617.0–141620.0	0.37	116	0.04 (64%)	14.50	88	0.66
12 <sup>I</sup>	20161106/084056.0–084100.0	0.26	103	0.66 (71%)	22.46	88	0.56
13 <sup>I</sup>	20161112/174846.0–174849.0	0.34	110	0.05 (50%)	16.68	87	0.64
14 <sup>I</sup>	20161113/091039.0–091042.0	0.16	271	0.17 (54%)	28.24	89	0.58
15	20161219/141459.0–141502.0	0.28	106	0.05 (72%)	17.25	88	0.61
16	20170120/123204.0–123207.0	0.25	119	0.24 (69%)	28.10	88	0.62
17	20170122/104739.0–104742.0	0.14	43	0.01 (56%)	25.62	88	0.56
18*	20170617/202406.0–202409.0	2.12	910	0.001 (98%)	5.05	76	0.75
19*	20170619/094323.0–094325.5	11.47	594	0.001 (99%)	1.75	47	0.78
20*	20170703/052649.7–052650.4	0.46	245	0.01 (99%)	5.38	86	0.53
21 <sup>I</sup> *	20170703/052707.2–052707.8	1.05	627	0.03 (95%)	5.24	49	0.71
22*	20170726/000354.0–000402.0	1.52	243	−0.001 (99%)	4.98	79	0.76
23 <sup>I</sup> *	20170810/121830.0–121838.0	3.16	599	−0.001 (99%)	3.92	69	0.81
24*	20170619/094325.7–094327.7	1.24	99	0.002 (99%)	5.18	84	0.81
25*	20170726/000347.0–000351.8	0.79	544	0.003 (97%)	6.35	80	0.70
26*	20180821/110100.5–110101.4	3.12	379	−0.001 (99%)	4.57	65	0.78

*Note.* Events 1 to 17 are the LHDWs in the vicinity and inside of magnetopause EDRs and events 18 to 26 marked by stars are magnetotail events. The plasma parameters for each event are presented. References to individual events published: Event 4 (Khotyaintsev et al., 2016), Event 7 (Yoo et al., 2020), Event 21 (Chen et al., 2020), Event 23 (Cozzani et al., 2021). Events 4, 5, 8, 9, 11, 12, 13, 14, 21 and 23 are inside of the EDR and they are marked with superscript *I*. The percentage values in  $\delta J_{\parallel} \delta E'_{\parallel}$  column indicates the percentage of power below 16.5 Hz relative to  $2f_{LH}$  limit.

samples/second) and burst magnetic field (128 samples/second) data. We average the power in the frequency range of  $[f_{\min}, 2f_{LH}]$  for each event with the minimum frequency of  $f_{\min} = 1$  Hz. The representative  $f_{LH}$  of each event is shown in Table 1.

Figure 1 shows an overview of event #5 in the magnetopause and event #18 in the magnetotail given in Table 1. The two events are chosen as they are representative of LHDWs in the magnetopause and LHDWs in the magnetotail. The intervals where the LHDWs are observed, are marked by the vertical dashed black lines in each plot in Figure 1. LHDWs are accompanied by fluctuations in both magnetic and electric fields near the lower hybrid frequency, and large measurements of  $\mathbf{J} \cdot \mathbf{E}'$  where  $\mathbf{J}$  is the current density and  $\mathbf{E}' = \mathbf{E} + \mathbf{V}_e \times \mathbf{B}$  is the electric field in electron reference frame. The  $\mathbf{J} \cdot \mathbf{E}'$  measures the energy exchange between particles and electromagnetic fields. For magnetopause events, we use FPI data to calculate the current density  $\mathbf{J}$  and for magnetotail events, we use the curlometer technique using four spacecraft to measure the current (Paschmann & Daly, 2000). Fast electric field with 32 samples per second, burst magnetic field with 128 samples per second and FPI electron burst data with 33 samples per second resolution are used to measure  $\mathbf{E}'$ . In order to remove the DC component of electromagnetic fields from energy transfer calculations, we apply a high pass filter with cut off

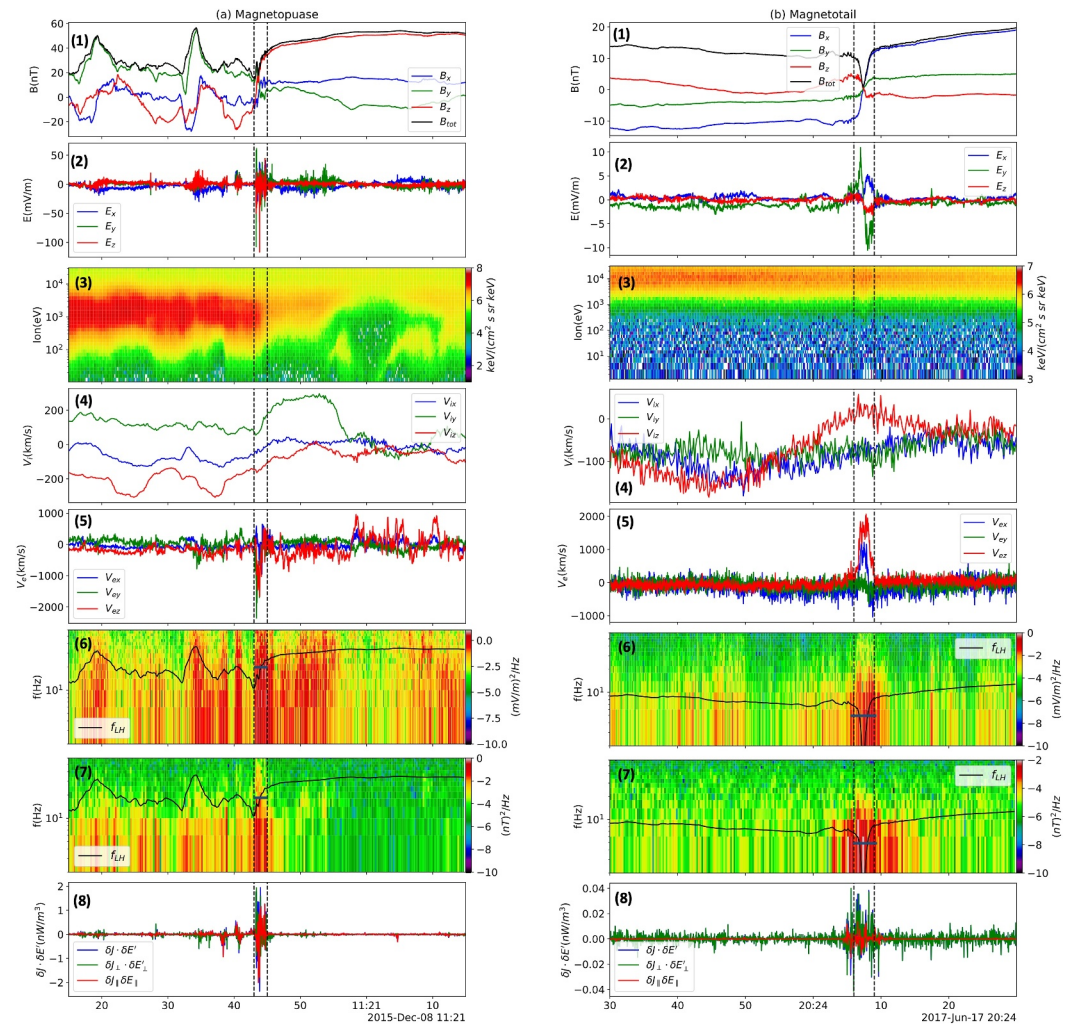


**Figure 1.** Overview of (a) magnetopause event #5 and (b) magnetotail event #18 with LHDWs using MMS1 data. The vertical black dashed lines show the interval of LHDWs observation. LHDWs are accompanied by fluctuations in magnetic and electric fields, wave power close to lower hybrid frequency and large measurements of energy transfer. Panels for both events are: (a) magnetic field, (b) electric field, (c) ion energy spectrogram, (d) ion velocity, (e) electron velocity, (f) electric field power  $|E|^2$  spectral density, (g) magnetic field power  $|B|^2$  spectral density and (h)  $\delta\mathbf{J} \cdot \delta\mathbf{E}'$  showing contribution of the LHDWs in energy transfer. The blue lines in the LHDW intervals in panels f and g are the mean LHDW frequency for each event.

frequency of  $f_{cut-off} = 1$  Hz to both  $\mathbf{J}$  and  $\mathbf{E}'$ . The high pass filter removes the energy transfer due to the reconnection electromagnetic fields. Now, the high pass filtered  $\delta\mathbf{J} \cdot \delta\mathbf{E}'$  only shows the contribution of the LHDWs in the energy transfer as presented in panel 8 of Figure 1. The  $\delta\mathbf{J} \cdot \delta\mathbf{E}'$  is measured with 30 ms resolution (FPI burst electron resolution measurement) or 33 Hz, corresponding to a Nyquist frequency of 16.5 Hz which is close to the lower hybrid frequency range for most of the events. The limitation in upper bound frequency in measurement of  $\delta\mathbf{J} \cdot \delta\mathbf{E}'$  comes from  $\mathbf{J}$  resolution in FPI data. The percentage of electric field power below 16.5 Hz compared to power below  $2f_{LH}$  frequency is included in  $\delta J_{\parallel} \delta E'_{\parallel}$  column. All of the events show that 50% or more of the electric field power is below 16.5 Hz.

### 3. Results

#### 3.1. Correlation Study: LHDW Type

Previously, it was suggested (Carter et al., 2001; Daughton, 2003; Davidson et al., 1977) that plasma beta plays in an important role in the stability of LHDW. More recently, Yoo et al. (2020) suggests that the nature of LHDW, or

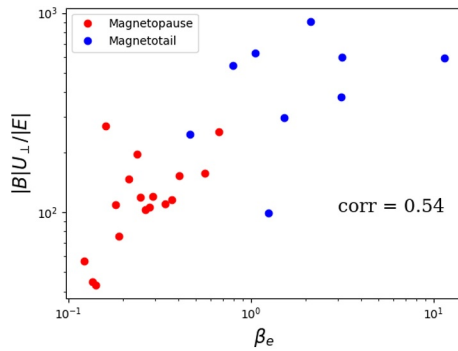


**Figure 2.** Relation between  $|B|U_{\perp}/|E|$  and  $\beta_e$ . Correlation study of how LHDW type, quantified by  $|B|U_{\perp}/|E|$ , is affected by  $\beta_e$ . Magnetopause data is shown in red and magnetotail data in blue. The figure shows a positive correlation suggesting that LHDWs become more electromagnetic as  $\beta_e$  increases.

equivalently ES-LHDW versus EM-LHDW, is determined by electron beta,  $\beta_e$  based on a single reconnection event. To quantify the nature of LHDW, we use the expression  $|B|U_{\perp}/|E|$  where  $|B|$  and  $|E|$  are wave amplitude in magnetic and electric fields, respectively. The ratio  $|B|/|E|$  is simply a measure of how electromagnetic the wave is. This ratio is normalized by the  $U_{\perp}$  or perpendicular relative drift between ions and electrons,  $V_e - V_i$ , which serves as the free energy source of LHDWs, and is a good proxy of the wave phase velocity (Ji et al., 2005). Therefore, this dimensionless quantity is an effective measure of the relative importance of magnetic field oscillations to their electric field counterpart in the LHDW. We measure the mean wave power  $|E|^2$  and  $|B|^2$  for the frequency range in  $[1, 2f_{LH}]$  for each event for the duration of the LHDW interval shown in Table 1.  $f_{LH}$  is the mean lower hybrid frequency in the LHDW interval. The table lists a column for  $f_{LH}$ , a column for  $\beta_e$ , and a column for  $|B|U_{\perp}/|E|$ , respectively.

Figure 2 shows a clear positive correlation between  $|B|U_{\perp}/|E|$  and  $\beta_e$  with a Pearson correlation coefficient of 0.54. This suggests that as  $\beta_e$  increases, the

LHDW becomes more electromagnetic in nature. Blue circle indicate magnetotail events and red circles are the magnetopause events. The magnetopause has relatively lower  $\beta_e$  values while magnetotail events have higher  $\beta_e$  values. These results suggest that the relatively lower  $\beta_e$  in the magnetopause causes LHDWs observed to be quasi-electrostatic in nature. This is in agreement with previous work on a particular reconnection event at magnetopause that LHDWs are generally more quasi-electrostatic at low  $\beta_e$  while more quasi-electromagnetic at high  $\beta_e$  (Yoo et al., 2020). This shows that the plasma parameters affect the characteristics of the LHDWs observed, thus, the role played by LHDWs may differ at each location.

### 3.2. Correlation Study: Energy Transfer

We conduct a correlation study between electric and magnetic field wave powers with  $\delta\mathbf{J} \cdot \delta\mathbf{E}'$  where LHDWs are present to study the energy transfer by these waves near and inside the EDRs.  $\delta\mathbf{J} \cdot \delta\mathbf{E}'$  quantifies the energy transfer between electromagnetic fields and particles in the electron rest frame (Zenitani et al., 2011). Positive  $\delta\mathbf{J} \cdot \delta\mathbf{E}'$  means that energy is transferred from fields to particles and a negative sign means the opposite.

Figures 3a–3c shows scatter plots of  $\delta\mathbf{J} \cdot \delta\mathbf{E}'$ ,  $\delta\mathbf{J}_{\perp} \cdot \delta\mathbf{E}'_{\perp}$  and  $\delta\mathbf{J}_{\parallel} \cdot \delta\mathbf{E}'_{\parallel}$  versus  $|E|^2$  in the left column and the same energy transfer versus  $|B|^2$  in Figures 3d and 3e in the right column. There is a general trend that higher energy transfer takes place when the wave powers are larger, for both electric and magnetic fields. This supports the notion that LHDW contributes to magnetic energy dissipation which includes electron heating (Yoo et al., 2024). Another trend from Figure 3 is that the energy transfer is generally higher for magnetopause events (red circles with the mean value of  $0.15 \text{ nW/m}^3$ ) than magnetotail events (blue circles with the mean value of  $0.004 \text{ nW/m}^3$ ). Since LHDW in magnetopause is generally more electrostatic in nature at low  $\beta_e$ , this trend is also consistent with the recent results from the laboratory (Yoo et al., 2024) where electrostatic LHDW are detected at low  $\beta_e$  producing anomalous resistivity.

However, it should be noted that  $\delta\mathbf{J} \cdot \delta\mathbf{E}'$  is overall higher in magnetopause events due to higher density and stronger magnetic field. Currently, there is not enough data to show clearly whether dissipating magnetic energy by LHDW during reconnection is more influenced by the wave being quasi-electrostatic or by simply having larger wave power.

In addition, there are some trends in directional dependence for magnetic energy dissipation. On average for all magnetopause events (red circles), the parallel contribution of the energy transfer is higher and more positive according to Figures 3c and 3f with the mean value of  $0.14 \text{ nW/m}^3$ . This is in contrast to the perpendicular contribution shown as red circles in Figures 3b and 3e where the energy transfer has larger scatters with both positive and negative signs and the mean value is  $0.01 \text{ nW/m}^3$ . Same things can be said for the magnetotail events, shown in the Figures 3b, 3c, 3e, and 3f as blue circles, but with smaller scatters. For magnetotail events, the mean value for perpendicular terms is  $-0.001 \text{ nW/m}^3$  and for parallel terms mean value, we get  $0.005 \text{ nW/m}^3$ .

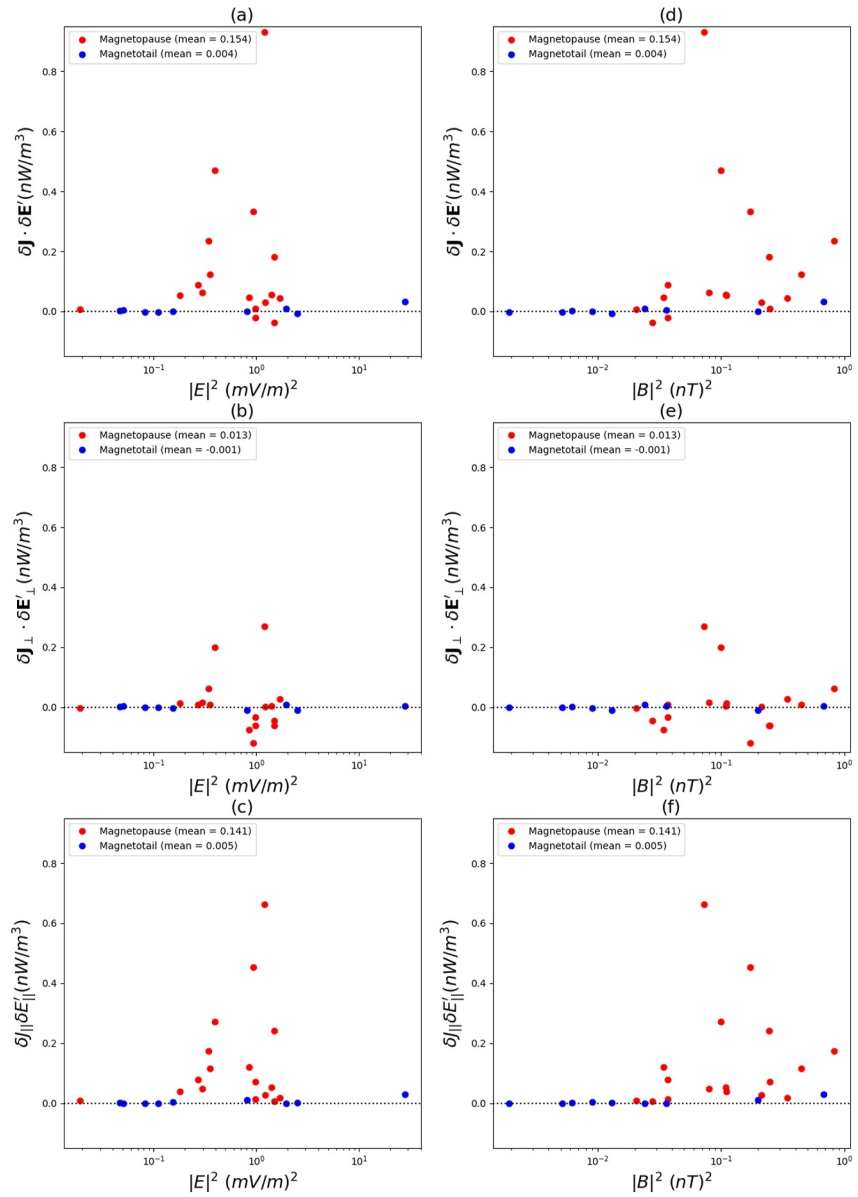


**Figure 3.** Energy transfer versus electric and magnetic field power. Magnetopause data is shown in red and magnetotail data in blue. (a)  $\delta \mathbf{J} \cdot \delta \mathbf{E}'$ , (b)  $\delta \mathbf{J}_{\perp} \cdot \delta \mathbf{E}'_{\perp}$ , (c)  $\delta J_{\parallel} \delta E'_{\parallel}$  versus  $|E|^2$  and (d)  $\delta \mathbf{J} \cdot \delta \mathbf{E}'$ , (e)  $\delta \mathbf{J}_{\perp} \cdot \delta \mathbf{E}'_{\perp}$ , and (f)  $\delta J_{\parallel} \delta E'_{\parallel}$  versus  $|B|^2$ . There is higher energy exchange at magnetopause events where LHDWs are more electrostatic. The mean values for each plot is shown for both magnetopause and magnetotail events. On average, the energy exchange is mostly in parallel direction as the mean values for parallel terms are much larger than the mean values of perpendicular energy transfer terms.

#### 4. Dispersion Relation Analysis

In order to aid our understanding of the LHDWs properties such as direction of propagation and their wave-number, we use a theoretical model of LHDW dispersion relation developed by Yoo et al. (2020). This model can predict additional LHDW properties that may help explain the above analyses but is difficult to obtain from the spacecraft data. The LHDW properties include the propagation direction, wavenumber magnitude, and growth rate.

The linear dispersion relation model is based on the work developed by Ji et al. (2005). Yoo et al. (2020) have improved the model to include the electron heat flux for better modeling of the perturbed parallel electron pressure, electron temperature anisotropy, parallel electron flow, and independent computation of the perturbed

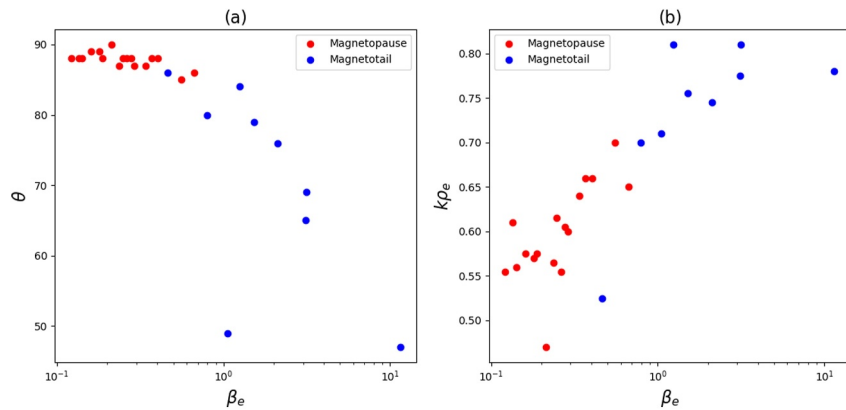


**Figure 4.** (a) Relation between direction of propagation and  $\beta_e$  and (b) relation between wavenumber and  $\beta_e$ . Magnetopause data is shown in red and magnetotail data in blue. As LHDWs become more electromagnetic for higher  $\beta_e$ , their direction of propagation becomes more oblique. LHDWs in magnetopause are more perpendicular propagating while the waves in magnetotail are more oblique. Lower  $\beta_e$  and magnetopause events have lower wavenumbers and larger  $\beta_e$  LHDWs have larger wavenumbers.

electron density for electrostatic effects. Using this model, the dispersion relation can be calculated as a function of the angle between the wave vector and magnetic field.

We use this model to calculate the propagation angle with respect to magnetic field and the wavenumber magnitude at the peak growth rate for each LHDW event. We use the averaged plasma parameters measured by MMS during each LHDW interval as input to the dispersion relation model. The input parameters are magnetic field, density, ion temperature, perpendicular and parallel electron temperatures and relative drift between ions and electrons. The model results are shown in Table 1 in columns  $\theta$  (propagation angle) and  $k\rho_e$  (normalized wavenumber by electron gyro-radius  $\rho_e$  calculated by using perpendicular electron temperature). Figure 4a shows the relation between the propagation direction and  $\beta_e$ . Magnetopause data is shown in red and magnetotail data in blue. As LHDWs become more electromagnetic for higher  $\beta_e$ , their direction of propagation becomes more oblique, consistent with the previous measurements (Ji et al., 2004; Yoo et al., 2020). LHDWs in magnetopause are more perpendicular propagating while the waves in magnetotail are more oblique. Figure 4b displays the relation between wavenumber magnitude and  $\beta_e$ . LHDW at lower  $\beta_e$  in the magnetopause events have lower wavenumbers or longer wavelengths while LHDW at larger  $\beta_e$  in the magnetotail events have larger wavenumbers or shorter wavelengths. Note that this result differs from the previous report (Daughton, 2003). The normalized wavenumber, however, stays within 0.5–0.8 range for all LHDW types. Daughton (2003) results are based on the upstream asymptotic magnetic field and the temperature at the current sheet mid-plane, while our plasma parameters are calculated at the interval of LHDWs and  $\rho_e$  is calculated using total magnetic field. Therefore, there may be uncertainties when comparing properties like  $k\rho_e$ . Since  $\rho_e$  here is based on the total magnetic field, a strong guide field can reduce  $\rho_e$  for the same reconnecting magnetic field. So even if the normalized  $k\rho_e$  decreases,  $k$  alone may not decrease that much.

Regardless its nature, however, the LHDW growth rate is controlled by the relative drift between ions and electrons along the direction perpendicular to the magnetic field, which is the free energy source related to electron density or pressure gradient. Figure 5a displays the relation between growth rate normalized to the lower hybrid angular frequency,  $\gamma/\omega_{LH}$  ( $\omega_{LH} = 2\pi f_{LH}$ ), and the normalized relative drift,  $U_{\perp}/C_s$  (with  $C_s = \sqrt{2K_B T_e/m_i}$ ). Magnetopause events have lower normalized growth rates and magnetotail LHDWs have larger normalized growth rates. This is expected since magnetopause events have smaller normalized drift speeds.

## 5. Effects of LHDW on Magnetic Reconnection

Figure 3 suggests that magnetic energy dissipation is related to the LHDW power. With the growth rate available for each event per Figure 5a, some simple but more quantitative tests are possible on the effects of LHDW on magnetic reconnection, as shown below.

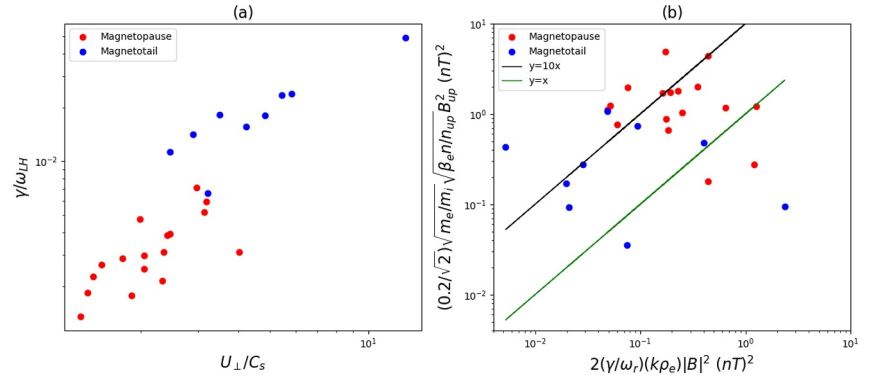


**Figure 5.** (a) Relation between normalized growth rate  $\gamma/\omega_{LH}$  and relative drift  $U_{\perp}/C_s$ . Magnetopause data is shown in red and magnetotail data in blue. As LHDWs become more electromagnetic for higher  $U_{\perp}/C_s$ , they have higher growth rates. (b) Both sides of Equation 2 are plotted to examine the effects of LHDW on magnetic reconnection via wave friction force.  $B_{up}$  ( $n_{up}$ ) is calculated by taking the mean value of reversing magnetic field component (ion density) on both sides of the LHDW interval. We move 2 s from the LHDW interval on each side for the 5 s average window. In panel (b), Green line represents  $y = x$ , indicating events that their LHDW power is sufficient to support the reconnection electric field. The black line shows  $y = 10x$  where the LHDW power is only 10% of what is needed to support reconnection electric field.

A simple but physically intuitive approach (Ji et al., 2004) is taken to evaluate LHDW energy balance during nonlinear saturation in steady state,

$$2\gamma\mathcal{E} + 2\gamma_{NL}\mathcal{E} = 0, \quad (1)$$

where  $\gamma_{NL}$  is “an effective growth rate” of LHDW due to nonlinear saturation.  $\mathcal{E}$  is the total wave energy and dominated by the wave magnetic field energy,  $\mathcal{E} = 2(\epsilon_0|E|^2/2 + |B|^2/2\mu_0) \approx |B|^2/\mu_0$ . Equation 1 can be understood as in the following. Without nonlinear saturation, the wave would continuously grow without bound. In order to achieve steady state over time, the nonlinear saturation needs to balance the linear growth of the wave. The quantity  $\gamma_{NL}$  in Equation 1 is introduced to represent the strength of the nonlinear saturation in the form of “an effective growth rate.” From Equation 1, we have  $\gamma_{NL} = -\gamma$ , and because  $\gamma > 0$ , then  $\gamma_{NL} < 0$ , which represents “effective nonlinear wave damping”, presumably by dissipating (perpendicular) electric current and thus magnetic energy to plasma.

As described in Ji et al. (2004), the momentum per unit volume carried by the LHDW is simply  $k\mathcal{E}/\omega_r$ , where  $k$  is the wavenumber vector and  $\omega_r$  is real angular frequency. The growth of the wave momentum (at the rate of  $2\gamma$ ) is at the expense of the momentum loss between ions and electrons due to the total momentum conservation. This manifests as a friction force between ions and electrons or resistivity by the waves,  $2\gamma_{NL}k\mathcal{E}/\omega_r = -2\gamma k\mathcal{E}/\omega_r$ . This friction force can be compared with what is needed to support the reconnection electric field,  $E_{rec} \approx 0.2B_{up}V_A$ , where the reconnection rate is assumed to be 0.2 (Liu et al., 2024; Pritchard et al., 2023),  $B_{up}$  is the upstream reconnecting magnetic field component, and  $V_A = B_{up}/\sqrt{\mu_0 m_i n_{up}}$  is Alfvén speed. Here  $m_i$  is ion mass and  $n_{up}$  is plasma density at the location of  $B_{up}$ . Equating the wave friction force,  $2\gamma/\omega_r k\mathcal{E}$ , with what is needed for reconnection,  $enE_{rec}$ , yields

$$\frac{0.2}{\sqrt{2}} \sqrt{\frac{m_e}{m_i} \frac{n}{n_{up}}} B_{up}^2 = 2 \left( \frac{\gamma}{\omega_r} \right) (k\rho_e) |B|^2, \quad (2)$$

where  $\mu_0\rho_e$  was multiplied on both sides of the equation for simplification,  $m_e$  is the electron mass,  $n$  is the density at the LHDW interval and  $\rho_e$  is calculated using the perpendicular electron temperature.

Both sides of Equation 2 are plotted in Figure 5b where exists a general positive correlation.  $B_{up}$  ( $n_{up}$ ) is calculated by taking the mean value of reversing magnetic field component (ion density) on both sides of the LHDW interval. Interesting, there are a subset of events (along  $y = x$ , green line) exhibiting similar magnitudes for both sides, indicating their LHDW power is sufficient to support reconnection electric field. In contrast, there

are more events (along  $y = 10x$ , black line) where the LHDW power is only 10% of what is needed to support reconnection electric field. However, in either case there is a positive correlation suggesting possible roles played by LHDW in reconnection, as recently reported from the laboratory experiment (Yoo et al., 2024).

## 6. Conclusion and Discussion

A survey analysis of LHDWs events near and inside the EDRs in magnetopause and magnetotail reconnection has been performed using MMS observations and a linear dispersion relation model. Time averaged plasma parameters are calculated for LHDW observation periods in 17 magnetopause reconnection events and 9 magnetotail events recorded by MMS. Results show that  $\beta_e$  is positively correlated with the ratio of  $|B|U_{\perp}/|E|$ , suggesting  $\beta_e$  is related to whether a LHDW is quasi-electromagnetic (EM-LHDW) or quasi-electrostatic (ES-LHDW). This significantly extended prior results (Yoo et al., 2020) based on a single reconnection event, adding new physics insights to a large body of past work on LHDW during reconnection in the laboratory, as reviewed recently by Ji et al. (2023). More specifically, this work significantly broadened the parameter space by using events from both magnetopause and magnetotail, and thus, enabled identifying the controlling parameter to better organize the reconnection events that contain LHDW.

Furthermore, a correlation study between electric and magnetic wave powers ( $|E|^2$  and  $|B|^2$ ) and energy transfer ( $\delta\mathbf{J} \cdot \delta\mathbf{E}'$ ) is conducted. Our results show that the energy transfer  $\delta\mathbf{J} \cdot \delta\mathbf{E}'$  is higher when LHDWs are more electrostatic, and the transfer is larger and positive in the parallel direction of magnetic field via  $\delta J_{\parallel} \delta E_{\parallel}$  than in the perpendicular direction via  $\delta J_{\perp} \cdot \delta E'_{\perp}$ . In addition,  $\delta\mathbf{J} \cdot \delta\mathbf{E}'$  is overall higher in magnetopause events than in magnetotail events.

A linear dispersion relation of LHDW (Yoo et al., 2020) is used to calculate the propagation angle and the normalized wavenumber for each reconnection event. As LHDWs become more electromagnetic for higher  $\beta_e$ , their direction of propagation becomes more oblique, consistent with previous laboratory measurements (Ji et al., 2004). LHDWs in magnetopause are more perpendicular propagating while the waves in magnetotail are more oblique. The dispersion relation model results show that the normalized wavenumber for all LHDW types stays within 0.5–0.8 range. Linear dispersion relation model also predicts that  $U_{\perp}/C_s$  impacts the normalized growth rate of LHDWs. Larger values of  $U_{\perp}/C_s$  leads to larger normalized growth rates for these waves. Graham et al. (2022) evaluated anomalous terms associated with LHDWs, which showed that associated anomalous terms (resistivity and viscosity) canceled each other. Here, following Ji et al. (2004), we took a straightforward but quantitative approach. Using the calculated growth rates, a simple estimate on nonlinear effects of LHDW on reconnection indicates possibly important roles played by these wave in supporting reconnection electric field.

The results reported above clearly benefited from combining the MMS data from both magnetopause and magnetotail events, by significantly expanding the range of important parameters such as  $\beta_e$ . Many trends would not be clear if focusing on the events only one of these two locations. However, we still cannot delineate two factors contributing to magnetic energy transfer between LHDW being quasi-electrostatic and LHDW having large wave amplitudes in the magnetopause reconnection events. A similar comment can be made also about magnetotail events which are simultaneously being quasi-electromagnetic and having smaller wave amplitudes. Therefore, more reconnection events with LHDW activity should be collected to further improve our understanding.

Combining theory and observation also clearly improves our understanding of these waves. The linear LHDW dispersion relation used here is simple and provides physical insights that cannot be easily available from the data. It is useful even for nonlinear physics such as anomalous resistivity (Yoo et al., 2024). However, it has a severe limitation due to its assumption of a local slab model. The EDRs are typically on the order of electron scales so that the effects due to their global boundaries may not be negligible. Numerical simulation by Particle-In-Cell methods such as by Ng et al. (2023) should be used in junction to provide much needed further insights. In this study, we investigated the local microphysics of the LHDWs in the magnetopause and magnetotail reconnection but in the future work, LHDWs in other regions like dipolarization fronts (Hosner et al., 2024) and their correlation with global parameters like solar wind conditions and geomagnetic indices could be investigated.

Wave properties such as the wave vector and the angle of propagation can be estimated with multi-spacecraft methods such as multi-spacecraft interferometry (Graham et al., 2016). We have considered estimating the wave properties with the multi-spacecraft method for a future study and comparing the results with the linear

dispersion analysis for all events. The accuracy of the multi-spacecraft analysis depends on the tetrahedron quality and the analysis can be challenging for poor spacecraft correlation.

### Data Availability Statement

All the MMS data used in this work are available at the MMS data center in the link: <https://lasp.colorado.edu/mms/sdc/public/about/browse-wrapper/>. The data have been loaded, analyzed, and plotted using the PYSPEDAS software, which can be downloaded via the Downloads and Installation page (<https://github.com/spedas/pyspedas>).

### Acknowledgments

This work was supported by NASA Grant 80HQTR21T0060. The authors thank the MMS instrument teams for providing the data and the PYSPEDAS team for providing the data analysis tools. Izzy Thomas, Rahul Banka and Emma Schultz-Stachnik were supported by Princeton Plasma Physics Laboratory (PPPL) Science Undergraduate Laboratory Internship (SULI). Alma Alex was supported by PPPL High School Internship Program. The authors would like to thank Erik Ji and Maitian Sha for their contributions on python coding and data analysis.

### References

- Bale, S., Mozer, F., & Phan, T. (2002). Observation of lower hybrid drift instability in the diffusion region at a reconnecting magnetopause. *Geophysical Research Letters*, *29*(24), 2180. <https://doi.org/10.1029/2002GL016113>
- Carter, T., Ji, H., Trintchouk, F., Yamada, M., & Kulsrud, R. (2001). Measurement of lower-hybrid drift turbulence in a reconnecting current sheet. *Physical Review Letters*, *88*(1), 015001. <https://doi.org/10.1103/PhysRevLett.88.015001>
- Cattell, C. A., & Mozer, F. S. (1986). Experimental determination of the dominant wave mode in the active near-earth magnetotail. *Geophysical Research Letters*, *13*(3), 221–224. <https://doi.org/10.1029/GL013i003p00221>
- Chen, L.-J., Wang, S., Le Contel, O., Rager, A., Hesse, M., Drake, J., et al. (2020). Lower-hybrid drift waves driving electron nongyrotropic heating and vortical flows in a magnetic reconnection layer. *Physical Review Letters*, *125*(2), 025103. <https://doi.org/10.1103/PhysRevLett.125.025103>
- Cozzani, G., Khotyaintsev, Y. V., Graham, D. B., Egedal, J., André, M., Vaivads, A., et al. (2021). Structure of a perturbed magnetic reconnection electron diffusion region in the earth's magnetotail. *Physical Review Letters*, *127*(21), 215101. <https://doi.org/10.1103/PhysRevLett.127.215101>
- Daughton, W. (2003). Electromagnetic properties of the lower-hybrid drift instability in a thin current sheet. *Physics of Plasmas*, *10*(8), 3103–3119. <https://doi.org/10.1063/1.1594724>
- Davidson, R., & Gladd, N. (1975). Anomalous transport properties associated with the lower-hybrid drift instability. *Physics of Fluids*, *18*(10), 1327–1335. <https://doi.org/10.1063/1.861021>
- Davidson, R., Gladd, N., Wu, C., & Huba, J. (1977). Effects of finite plasma beta on the lower-hybrid drift instability. *The Physics of Fluids*, *20*(2), 301–310. <https://doi.org/10.1063/1.861867>
- Drake, J. F., Swisdak, M., Che, H., & Shay, M. A. (2006). Electron acceleration from contracting magnetic islands during reconnection. *Nature*, *443*(7111), 553–556. <https://doi.org/10.1038/nature05116>
- Ergun, R. E., Tucker, S., Westfall, J., Goodrich, K. A., Malaspina, D. M., Summers, D., et al. (2016). The Axial double probe and fields signal processing for the MMS mission. *Space Science Reviews*, *199*(1–4), 167–188. <https://doi.org/10.1007/s11214-014-0115-x>
- Graham, D. B., Khotyaintsev, Y. V., André, M., Vaivads, A., Divin, A., Drake, J. F., et al. (2022). Direct observations of anomalous resistivity and diffusion in collisionless plasma. *Nature Communications*, *13*(1), 2954. <https://doi.org/10.1038/s41467-022-30561-8>
- Graham, D. B., Khotyaintsev, Y. V., Norgren, C., Vaivads, A., André, M., Drake, J. F., et al. (2019). Universality of lower hybrid waves at earth's magnetopause. *Journal of Geophysical Research: Space Physics*, *124*(11), 8727–8760. <https://doi.org/10.1029/2019JA027155>
- Graham, D. B., Khotyaintsev, Y. V., Vaivads, A., & André, M. (2016). Electrostatic solitary waves and electrostatic waves at the magnetopause. *Journal of Geophysical Research: Space Physics*, *121*(4), 3069–3092. <https://doi.org/10.1002/2015JA021527>
- Hosner, M., Nakamura, R., Schmid, D., Nakamura, T. K. M., Panov, E. V., Volwerk, M., et al. (2024). Reconnection inside a dipolarization front of a diverging earthward fast flow. *Journal of Geophysical Research: Space Physics*, *129*(1), e2023JA031976. <https://doi.org/10.1029/2023JA031976>
- Ji, H., & Daughton, W. (2011). Phase diagram for magnetic reconnection in heliophysical, astrophysical, and laboratory plasmas. *Physics of Plasmas*, *18*(11), 111207. <https://doi.org/10.1063/1.3647505>
- Ji, H., Daughton, W., Jara-Almonte, J., Le, A., Stanier, A., & Yoo, J. (2022). Magnetic reconnection in the era of exascale computing and multiscale experiments. *Nature Reviews Physics*, *4*(4), 263–282. <https://doi.org/10.1038/s42254-021-00419-x>
- Ji, H., Kulsrud, R., Fox, W., & Yamada, M. (2005). An obliquely propagating electromagnetic drift instability in the lower hybrid frequency range. *Journal of Geophysical Research*, *110*(A8). <https://doi.org/10.1029/2005JA011188>
- Ji, H., Terry, S., Yamada, M., Kulsrud, R., Kuritsyn, A., & Ren, Y. (2004). Electromagnetic fluctuation during fast reconnection in a laboratory plasma. *Physical Review Letters*, *92*(11), 115001. <https://doi.org/10.1103/PhysRevLett.92.115001>
- Ji, H., Yoo, J., Fox, W., Yamada, M., Argall, M., Egedal, J., et al. (2023). Laboratory study of collisionless magnetic reconnection. *Space Science Reviews*, *219*(8), 76. <https://doi.org/10.1007/s11214-023-01024-3>
- Khotyaintsev, Y. V., Graham, D. B., Norgren, C., Eriksson, E., Li, W., Johlander, A., et al. (2016). Electron jet of asymmetric reconnection. *Geophysical Research Letters*, *43*(11), 5571–5580. <https://doi.org/10.1002/2016GL069064>
- Khotyaintsev, Y. V., Graham, D. B., Norgren, C., & Vaivads, A. (2019). Collisionless magnetic reconnection and waves: Progress review. *Frontiers in Astronomy and Space Sciences*, *6*, 70. <https://doi.org/10.3389/fspas.2019.00070>
- Lindqvist, E. A. P.-A., Olsson, G., Torbert, R. B., King, B., Granoff, M., Rau, D., et al. (2016). The spin-plane double probe electric field instrument for mms. *Space Science Reviews*, *199*(1–4), 137–165. <https://doi.org/10.1007/s11214-014-0116-9>
- Liu, Y.-H., Hesse, M., Genestreti, K., Nakamura, R., Burch, J., Cassak, P., et al. (2024). Ohm's Law, the reconnection rate, and energy conversion in collisionless magnetic reconnection. *arXiv e-Prints*. <https://doi.org/10.48550/arXiv.2406.00875>
- Ng, J., Yoo, J., Chen, L. J., Bessho, N., & Ji, H. (2023). 3D simulation of lower-hybrid drift waves in strong guide field asymmetric reconnection in laboratory experiments. *Physics of Plasmas*, *30*(4), 042101. <https://doi.org/10.1063/5.0138278>
- Norgren, C., Vaivads, A., Khotyaintsev, Y. V., & Andre, M. (2012). Lower hybrid drift waves: Space observations. *Physical Review Letters*, *109*(5), 055001. <https://doi.org/10.1103/PhysRevLett.109.055001>
- Paschmann, G., & Daly, P. W. (2000). *Analysis methods for multi-spacecraft data*. The International Space Science Institute.
- Pollock, C., Moore, T., Jacques, A., Burch, J., Gliese, U., Saito, Y., et al. (2016). Fast plasma investigation for magnetospheric multiscale. *Space Science Reviews*, *199*(1–4), 331–406. <https://doi.org/10.1007/s11214-016-0245-4>

- Pritchard, K. R., Burch, J. L., Fuselier, S. A., Genestreti, K. J., Denton, R. E., Webster, J. M., & Broll, J. M. (2023). Reconnection rates at the earth's magnetopause and in the magnetosheath. *Journal of Geophysical Research: Space Physics*, *128*(9). <https://doi.org/10.1029/2023JA031475>
- Russell, C. T., Anderson, B. J., Baumjohann, W., Bromund, K. R., Dearborn, D., Fischer, D., et al. (2016). The magnetospheric multiscale magnetometers. *Space Science Reviews*, *199*(1–4), 189–256. <https://doi.org/10.1007/s11214-014-0057-3>
- Shinohara, I., Nagai, T., Fujimoto, M., Terasawa, T., Mukai, T., Tsuruda, K., & Yamamoto, T. (1998). Low frequency electromagnetic turbulence observed near the substorm onset site. *Journal of Geophysical Research*, *103*(A9), 20365–20388. <https://doi.org/10.1029/98ja01104>
- Wang, S., Chen, L.-J., Bessho, N., Ng, J., Hesse, M., Graham, D. B., et al. (2022). Lower-hybrid wave structures and interactions with electrons observed in magnetotail reconnection diffusion regions. *Journal of Geophysical Research: Space Physics*, *127*(5), e2021JA030109. <https://doi.org/10.1029/2021JA030109>
- Webster, J. M., Burch, J. L., Reiff, P. H., Daou, A. G., Genestreti, K. J., Graham, D. B., et al. (2018). Magnetospheric multiscale dayside reconnection electron diffusion region events. *Journal of Geophysical Research: Space Physics*, *123*(6), 4858–4878. <https://doi.org/10.1029/2018JA025245>
- Yamada, M., Kulsrud, R., & Ji, H. (2010). Magnetic reconnection. *Reviews of Modern Physics*, *82*(1), 603–664. <https://doi.org/10.1103/RevModPhys.82.603>
- Yoo, J., Ji, J.-Y., Ambat, M. V., Wang, S., Ji, H., Lo, J., et al. (2020). Lower hybrid drift waves during guide field reconnection. *Geophysical Research Letters*, *47*(21), e2020GL087192. <https://doi.org/10.1029/2020GL087192>
- Yoo, J., Ng, J., Ji, H., Bose, S., Goodman, A., Alt, A., et al. (2024). Anomalous resistivity and electron heating by lower hybrid drift waves during magnetic reconnection with a guide field. *Physical Review Letters*, *132*(14), 145101. <https://doi.org/10.1103/PhysRevLett.132.145101>
- Zenitani, S., Hesse, M., Klimas, A., & Kuznetsova, M. (2011). New measure of the dissipation region in collisionless magnetic reconnection. *Physical Review Letters*, *106*(19), 195003. <https://doi.org/10.1103/PhysRevLett.106.195003>
- Zhou, M., Deng, X. H., Li, S. Y., Pang, Y., Vaivads, A., Rème, H., et al. (2009). Observation of waves near lower hybrid frequency in the reconnection region with thin current sheet. *Journal of Geophysical Research*, *114*(A2), 2216. <https://doi.org/10.1029/2008JA013427>